CLEO CONF 04-11
ICHEP04 ABS11-0776

# Measurement of $\mathcal{B}(D^+ \to \mu^+\nu)$ and the Pseudoscalar Decay Constant $f_{D^+}$*

D. Besson,[1] K. Y. Gao,[2] D. T. Gong,[2] Y. Kubota,[2] B.W. Lang,[2] S. Z. Li,[2] R. Poling,[2] A. W. Scott,[2] A. Smith,[2] C. J. Stepaniak,[2] J. Urheim,[2] Z. Metreveli,[3] K. K. Seth,[3] A. Tomaradze,[3] P. Zweber,[3] J. Ernst,[4] A. H. Mahmood,[4] H. Severini,[5] D. M. Asner,[6] S. A. Dytman,[6] S. Mehrabyan,[6] J. A. Mueller,[6] V. Savinov,[6] Z. Li,[7] A. Lopez,[7] H. Mendez,[7] J. Ramirez,[7] G. S. Huang,[8] D. H. Miller,[8] V. Pavlunin,[8] B. Sanghi,[8] E. I. Shibata,[8] I. P. J. Shipsey,[8] G. S. Adams,[9] M. Chasse,[9] M. Cravey,[9] J. P. Cummings,[9] I. Danko,[9] J. Napolitano,[9] D. Cronin-Hennessy,[10] C. S. Park,[10] W. Park,[10] J. B. Thayer,[10] E. H. Thorndike,[10] T. E. Coan,[11] Y. S. Gao,[11] F. Liu,[11] M. Artuso,[12] C. Boulahouache,[12] S. Blusk,[12] J. Butt,[12] E. Dambasuren,[12] O. Dorjkhaidav,[12] N. Menaa,[12] R. Mountain,[12] H. Muramatsu,[12] R. Nandakumar,[12] R. Redjimi,[12] R. Sia,[12] T. Skwarnicki,[12] S. Stone,[12] J. C. Wang,[12] K. Zhang,[12] S. E. Csorna,[13] G. Bonvicini,[14] D. Cinabro,[14] M. Dubrovin,[14] R. A. Briere,[15] G. P. Chen,[15] T. Ferguson,[15] G. Tatishvili,[15] H. Vogel,[15] M. E. Watkins,[15] N. E. Adam,[16] J. P. Alexander,[16] K. Berkelman,[16] D. G. Cassel,[16] V. Crede,[16] J. E. Duboscq,[16] K. M. Ecklund,[16] R. Ehrlich,[16] L. Fields,[16] L. Gibbons,[16] B. Gittelman,[16] R. Gray,[16] S. W. Gray,[16] D. L. Hartill,[16] B. K. Heltsley,[16] D. Hertz,[16] L. Hsu,[16] C. D. Jones,[16] J. Kandaswamy,[16] D. L. Kreinick,[16] V. E. Kuznetsov,[16] H. Mahlke-Krüger,[16] T. O. Meyer,[16] P. U. E. Onyisi,[16] J. R. Patterson,[16] D. Peterson,[16] J. Pivarski,[16] D. Riley,[16] J. L. Rosner,[16,†] A. Ryd,[16] A. J. Sadoff,[16] H. Schwarthoff,[16] M. R. Shepherd,[16] S. Stroiney,[16] W. M. Sun,[16] J. G. Thayer,[16] D. Urner,[16] T. Wilksen,[16] M. Weinberger,[16] S. B. Athar,[17] P. Avery,[17] L. Breva-Newell,[17] R. Patel,[17] V. Potlia,[17] H. Stoeck,[17] J. Yelton,[17] P. Rubin,[18] B. I. Eisenstein,[19] G. D. Gollin,[19] I. Karliner,[19] D. Kim,[19] N. Lowrey,[19] P. Naik,[19] C. Sedlack,[19] M. Selen,[19] J. J. Thaler,[19] J. Williams,[19] J. Wiss,[19] and K. W. Edwards[20]

(CLEO Collaboration)

[1]*University of Kansas, Lawrence, Kansas 66045*
[2]*University of Minnesota, Minneapolis, Minnesota 55455*
[3]*Northwestern University, Evanston, Illinois 60208*
[4]*State University of New York at Albany, Albany, New York 12222*
[5]*University of Oklahoma, Norman, Oklahoma 73019*
[6]*University of Pittsburgh, Pittsburgh, Pennsylvania 15260*
[7]*University of Puerto Rico, Mayaguez, Puerto Rico 00681*
[8]*Purdue University, West Lafayette, Indiana 47907*
[9]*Rensselaer Polytechnic Institute, Troy, New York 12180*
[10]*University of Rochester, Rochester, New York 14627*
[11]*Southern Methodist University, Dallas, Texas 75275*
[12]*Syracuse University, Syracuse, New York 13244*
[13]*Vanderbilt University, Nashville, Tennessee 37235*
[14]*Wayne State University, Detroit, Michigan 48202*
[15]*Carnegie Mellon University, Pittsburgh, Pennsylvania 15213*
[16]*Cornell University, Ithaca, New York 14853*
[17]*University of Florida, Gainesville, Florida 32611*

[18]*George Mason University, Fairfax, Virginia 22030*
[19]*University of Illinois, Urbana-Champaign, Illinois 61801*
[20]*Carleton University, Ottawa, Ontario, Canada K1S 5B6*
*and the Institute of Particle Physics, Canada*
(Dated: August 16, 2004)

## Abstract

In 60 pb$^{-1}$ of data taken on the $\psi(3770)$ resonance with the CLEO-c detector, we find 8 $D^+ \to \mu^+\nu$ event candidates that are mostly signal, containing only 1 estimated background. Using this statistically compelling sample, we measure preliminary values of $\mathcal{B}(D^+ \to \mu^+\nu) = (3.5 \pm 1.4 \pm 0.6) \times 10^{-4}$, and determine $f_{D^+} = (201 \pm 41 \pm 17)$ MeV.

---

*Submitted to the 32$^{\rm nd}$ International Conference on High Energy Physics, Aug 2004, Beijing
†On leave of absence from University of Chicago.

## I. INTRODUCTION

Measuring purely leptonic decays of heavy mesons allows the determination of meson decay constants, which connect measured quantities, such as the $B\bar{B}$ mixing ratio, to CKM matrix elements. Currently, it is not possible to determine $f_B$ experimentally from leptonic $B$ decays, so theoretical calculations of $f_B$ must be used. The most promising of these calculations involves lattice QCD [1] [2] [3], though there are other methods [4] [5] [6] [7] [8].

Measurements of pseudoscalar decay constants such as $f_{D^+}$ provide checks on these calculations and help discriminate among different models.


FIG. 1: The decay diagram for $D^+ \to \mu^+\nu$.

The decay diagram for $D^+ \to \mu^+\nu$ is shown in Fig. 1. The decay rate is given by [9]

$$\Gamma(D^+ \to l^+\nu) = \frac{G_F^2}{8\pi} f_{D^+}^2 m_l^2 M_{D^+} \left(1 - \frac{m_l^2}{M_{D^+}^2}\right)^2 |V_{cd}|^2 \quad , \tag{1}$$

where $M_{D^+}$ is the $D^+$ mass, $m_l$ is the mass of the final state lepton, $V_{cd}$ is a CKM matrix element equal to 0.2205 [10], and $G_F$ is the Fermi coupling constant. Various theoretical predictions of $f_{D^+}$ range from 190 MeV to 350 MeV. Because of helicity suppression, the electron mode $D^+ \to e^+\nu$ has a very small rate. The relative widths are $3.2 : 1 : 2.4 \times 10^{-5}$ for the $\tau^+\nu$, $\mu^+\nu$ and $e^+\nu$ final states, respectively. Unfortunately the mode with the largest branching fraction, $\tau^+\nu$, has at least two neutrinos in the final state and is difficult to detect.

## II. THE CLEO-C DETECTOR

The CLEO-c detector is equipped to measure the momenta and direction of charged particles, identify charged hadrons, detect photons and measure with good precision their directions and energies. Muons above 1.1 GeV can also be identified. The detector is almost cylindrically symmetric with everything but the muon detector inside a superconducting magnet coil run at a current that produces an almost uniform 1.0 T field. The detector consists of a six-layer wire drift chamber at small radius that is low mass, suitable for these relatively low energies. It is followed by a 47-layer drift chamber; both chambers use a gas mixture of 60% Helium and 40% Propane. These two devices measure charged track three-momenta with excellent accuracy. The drift chamber also measures energy loss, dE/dx, that is used to identify charged tracks below about 0.7 GeV/c. After the drift chamber there is a Ring Imaging Cherenkov Detector (RICH) [11] , that identifies charged particles over most of their momentum range. The RICH is surrounded by a Thallium doped CsI crystal array consisting of about 8000 tapered crystals 30 cm long and about 5x5 cm$^2$ at the rear.

## III. DATA SAMPLE AND SIGNAL SELECTION

In this study we use 60 pb$^{-1}$ of CLEO-c data recorded at the $\psi''$ resonance (3.770 GeV). These events consist of a mixture of $D^+D^-$, $D^o\overline{D}^o$ and continuum events. There also may be small amounts of $\tau^+\tau^-$ pairs and two-photon events.

We examine all the recorded events and retain those containing at least one charged $D$ candidate in the modes listed in Table I. The selection criteria are described in detail in what follows.

All acceptable track candidates must have a helical trajectory that approaches the event origin within a distance of 0.005 m in the azimuthal projection and 0.05 m in the polar projection, where the azimuthal projection is in the bend view of the solenoidal magnet. Each track must posses at least 50% of the hits expected to be on a track and its polar direction must have cosine with respect to the beam direction of magnitude $< 0.93$.

We use both charged particle ionization loss in the drift chamber (dE/dx) and RICH information to identify kaons and pions used to fully reconstruct $D$ mesons. The RICH is used for momenta larger than 0.55 GeV. Information on the angle of detected Cherenkov photons is translated into a Liklihood of a given photon being due to a particular particle. Contributions from all photons associated with a particular track are then summed to form an overall Liklihood denoted as $\mathcal{L}_i$ for each particle hypothesis. To differentiate between pion and kaon candidates, we use the difference: $-2\log(\mathcal{L}_\pi)+2\log(\mathcal{L}_K)$. Usually this cut is set at zero except for muon candidates where the difference between $-2\log(\mathcal{L}_\mu)+2\log(\mathcal{L}_K)$ is set at 10, to ensure a high, well understood efficiency. To utilize the dE/dx information we calculate $\sigma_\pi$ as the difference between the expected ionization loss for a pion and the measured loss divided by the measurement error. Similarly, $\sigma_K$ is defined in the same manner using the expected ionization for a kaon .

We use both the RICH and dE/dx information for $D^-$ meson tag candidate tracks in the following manner: (a) If neither the RICH nor dE/dx information is available, then the track is accepted as both a pion and a kaon candidate. (b) If dE/dx is available and RICH is not then we insist that pion candidates have $PID_{dE} = \sigma_\pi^2 - \sigma_K^2 < 0$ and kaon candidates have $PID_{dE} > 0$. (c) If RICH information is available and dE/dx is not available, then we require that $PID_{RICH} = -2\log(\mathcal{L}_\pi) + 2\log(\mathcal{L}_K) < 0$ for pions and $PID_{RICH} > 0$ for kaons. (d) If both dE/dx and RICH information are available, we require that $(PID_{dE} + PID_{RICH}) < 0$ for pions and $(PID_{dE} + PID_{RICH}) > 0$ for kaons.

We reconstruct $\pi^o$'s by first selecting photon candidates from energy deposits in the crystals not matched to charged tracks that have deposition patterns consistent with that expected for photons. Pairs of photon candidates are kinematically fit to the nominal $\pi^o$ mass. We require the pull, the difference between the raw and fit mass normalized by its uncertainty, to be less than three for accepted $\pi^o$ candidates.

$K_s^o$ are formed from a pair of charged pions which are kinematically fitted to come from a single vertex. We also require that the invariant mass of the two pions be within 4.5 times the width of the $K_s$ mass peak which is 0.004 GeV r.m.s.

## IV. RECONSTRUCTION OF CHARGED $D$ TAGGING MODES

Tagging modes are fully reconstructed by first evaluating the difference in the energy of the decay products with the beam energy. We then normally require the absolute value of this difference to be within 0.02 GeV of zero, approximately twice the r.m.s. width, and then look at the reconstructed $D^-$ beam constrained mass defined as

$$m_D = \sqrt{E_{beam}^2 - (\sum_i \overrightarrow{p}_i)^2}, \tag{2}$$

where $i$ runs over all the final state particles. We also use the charge-conjugate $D^+$ tags and search for $D^- \to \mu^-\overline{\nu}_\mu$; in the rest of this paper we will not mention the charge-conjugate modes explicitly, but they are always used.

The $m_D$ distribution for all $D^-$ tagging modes considered in this data sample are shown in Fig. 2 and listed in Table I along with the number of signal and background events. The event numbers are determined from fits of the $m_D$ distributions to Gaussian signal functions plus a background shape parameterized as $3^{rd}$ order polynomial for the $K^+\pi^-\pi^-\pi^o$, $K_s\pi^-\pi^-\pi^+$ and $K_s\pi^-\pi^o$ and from fits to double Gaussian signal functions plus $3^{rd}$ order polynomial for $K^+\pi^-\pi^-$ and $K_s\pi^-$ tags where we see a small tail on the higher mass side.

| Mode | Signal | Background |
|---|---|---|
| $K^+\pi^-\pi^-$ | $15188 \pm 233$ | $583 \pm 336$ |
| $K^+\pi^-\pi^-\pi^o$ | $4082 \pm 81$ | $1826 \pm 343$ |
| $K_s\pi^-$ | $2110 \pm 81$ | $251 \pm 19$ |
| $K_s\pi^-\pi^-\pi^+$ | $3975 \pm 81$ | $1880 \pm 342$ |
| $K_s\pi^-\pi^o$ | $3297 \pm 87$ | $4226 \pm 516$ |
| Sum | $28652 \pm 285$ | $8765 \pm 784$ |

TABLE I: Tagging modes and numbers of signal and background events determined from the fits shown in Fig.2.

Selecting those candidates within 3 r.m.s. widths of the $D^-$ mass reduces the signal number by 77 events giving a total of 28575±286 events used for further analysis.

## V. $D^+ \to \mu^+\nu_\mu$ SELECTION CRITERIA

To select $D^+ \to \mu^+\nu_\mu$ events we first reconstruct $D^-$ event candidates and then search for events with a single additional charged track presumed to be a $\mu^+$. Then we infer the existence of the neutrino by requiring a measured value near zero (the neutrino mass) of the missing mass squared (MM$^2$) defined as

$$\mathrm{MM}^2 = (E_{beam} - E_{\mu^+})^2 - \left(-\overrightarrow{p}_{D^-} - \overrightarrow{p}_{\mu^+}\right)^2, \tag{3}$$

where $\overrightarrow{p}_{D^-}$ is the three-momentum of the fully reconstructed $D^-$.

We need to restrict the sample to candidate $\mu^+\nu_\mu$ events resulting from the other $D$. Thus we wish to exclude events with more than one additional charged track, which we take to be the muon candidate, or with extra neutral energy. It is possible, in fact even likely, that the decay products of the tagging $D^-$ interact in the detector material, mostly the EM calorimeter and spray tracks and neutral energy back into the rest of the detector. To evaluate the size of these contributions we use a very pure sample of events obtained by finding fully reconstructed $D^o\overline{D}^o$ events. The numbers of these events in various decay modes are listed in Table II, we use a total of 782 events.

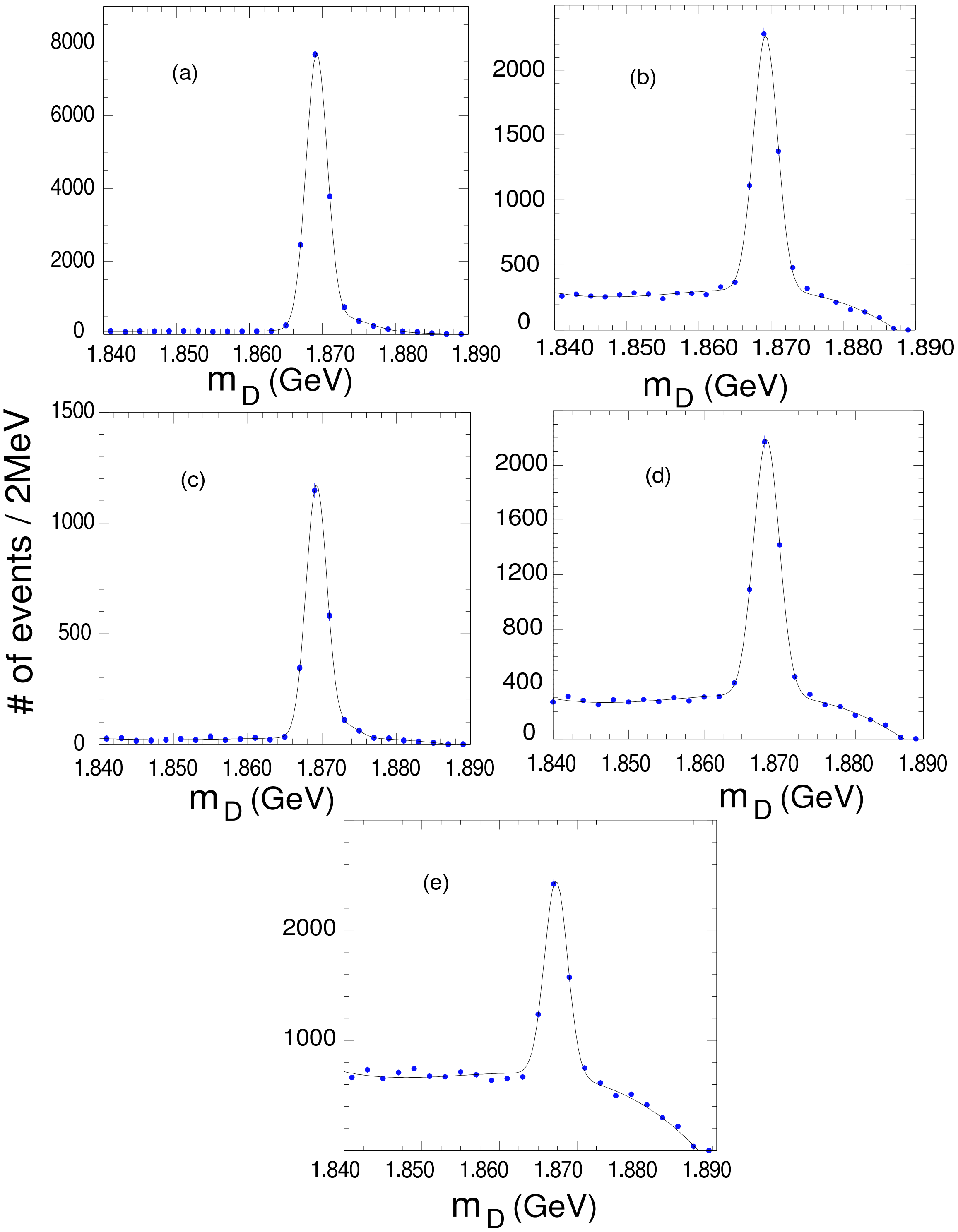


FIG. 2: Beam Constrained Mass distributions for different fully reconstructed $D^-$ decay candidates; the curves show the sum of Gaussian signal functions and $3^{rd}$ order polynomial background functions. A single signal Gaussian is used for all modes except for (a) and (c) where two Gaussians are used. (a) $D^- \to K^+\pi^-\pi^-$, (b) $D^- \to K^+\pi^-\pi^-\pi^0$, (c) $D^- \to K_s\pi^-$, (d) $D^- \to K_s\pi^-\pi^-\pi^+$ and (e) $D^- \to K_s\pi^-\pi^0$.(preliminary)

| Mode 1 | Mode 2 | # of events |
|---|---|---|
| $K^-\pi^+$ | $K^+\pi^-$ | 89 |
| $K^+\pi^-\pi^+\pi^-$ | $K^-\pi^+$ | 392 |
| $K^+\pi^-\pi^+\pi^-$ | $K^-\pi^+\pi^-\pi^+$ | 301 |

TABLE II: Fully reconstructed $D^o\overline{D}^o$ events

The number of interactions of particles with material and their consequences depend on the number of particles, the kind of particles and their momenta. Thus, the sum over these neutral $D$ decay modes isn't quite the same as the sum over the tagging $D^-$ decays, however the average over these modes is quite similar to the $D^-$ tagging modes for this level of statistics.

Extra tracks do appear in these $D^o\overline{D}^o$ events. None of these tracks, however, approach the main event vertex. Requiring that good tracks are within 0.05 m along the beam and 0.005 m perpendicular to the beam does not include any additional tracks from interactions in the material. $D^-$ tags with additional $K_s \to \pi^+\pi^-$ candidates are rejected.

In the $D^o\overline{D}^o$ events, energy in the calorimeter not matched to any of the charged tracks is shown in Fig. 3. Figure 3(a) shows the energy of the largest shower and 3(b) shows the total. We accept only as extra showers those that do not match a charged track within a connected region. A connected region is a group of adjacent crystals with energy depositions which are nearest neighbors. This suppresses a lot of hadronic shower fragments which would otherwise show up as unmatched showers. Hadronic interactions and very energetic $\pi^o$'s tend to produce one connected region with many clusters. For further analysis we require that the largest unmatched shower not to be larger than 250 MeV. This requirement is (93.5±0.9)% efficient for signal events.

The muon candidate is required to be within the barrel region of the detector $|\cos\theta| < 0.81$, where $\theta$ is the angle of the muon with respect to the beam electrons; this requirement insures that the MM$^2$ resolution is good as tracks at larger angles with respect to the beam are measured with poorer precision. In addition, this requirement helps reject background from the decay $D^+ \to \pi^+\pi^o$; this mode also gives a MM$^2$ near zero. Requiring the muon candidate in the barrel region (the $\pi^+$ in this case) avoids having the photons from this decay being lost in the transition region of the calorimeter between the barrel and the endcap, because the $\pi^o$ direction is almost directly opposite the $\pi^+$. Furthermore, the muon candidate is required not to be consistent with the kaon hypothesis using RICH information. Finally, we also require that the muon candidate deposits less than 300 MeV of energy in the calorimeter, characteristic of a minimum ionizing particle. This requirement is very efficient for real muons, and rejects about 40% of the pions as determined using a sample of reconstructed $D^o \to K^-\pi^+$ decays. Fig. 4 shows the muon deposited energy in the EM calorimeter both from data on $e^+e^- \to \mu^+\mu^-$ and from GEANT simulation of the same process. The Monte Carlo and data are in excellent agreement. We therefore use a GEANT simulation of $D^+ \to \mu^+\nu$ with lower energy muons to determine that the efficiency of the calorimeter energy cut is $(98.7 \pm 0.19)$%.

Table. III shows the properties of each muon candidate from the 8 events in the signal region. When evaluating MM$^2$ using equation 3 there are two important considerations that are not obvious. First of all, we explicitly need to take into account the crossing angle between the $e^+$ and $e^-$ beams. This angle is about 4 mrad, varying slightly run to run; we

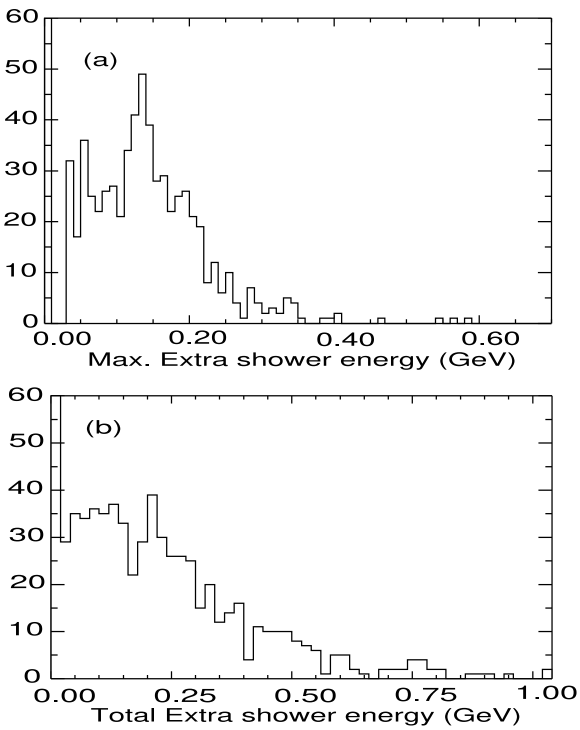


FIG. 3: Largest and Total Extra shower energies in the $D^o\overline{D}^o$ sample.

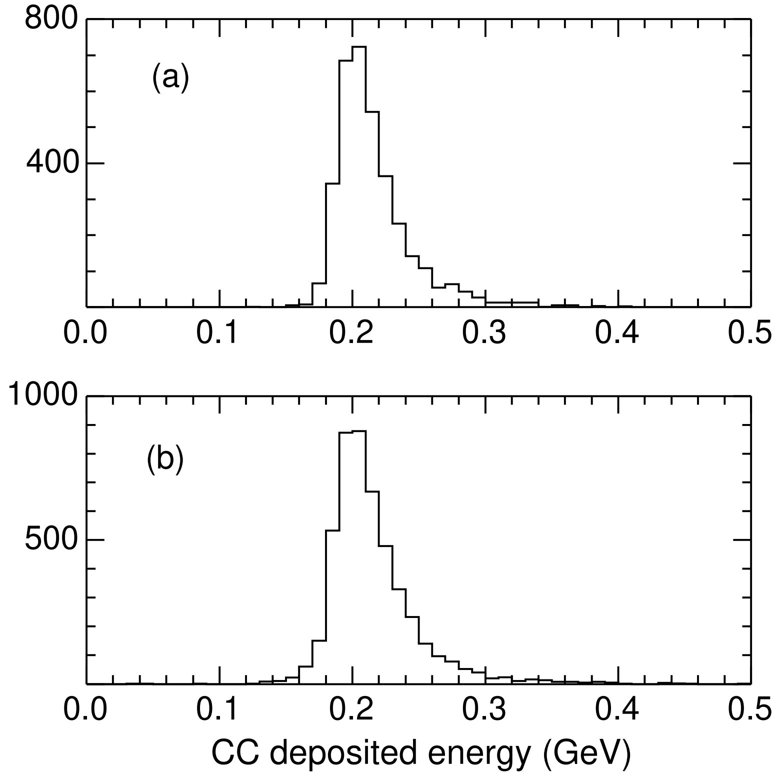


FIG. 4: Muon deposited energy in CC of Muon pairs from (a) DATA and (b) MC.

| Tag | $\text{MM}^2$ ($\text{GeV}^2$) | CC energy of $\mu^+$(GeV) | $-2\log(\mathcal{L}_K)$ | $-2\log(\mathcal{L}_\mu)$ | $\mu^\pm$ |
|---|---|---|---|---|---|
| $K\pi\pi\pi^o$ | 0.032 | 0.186 | -4.3 | -166.0 | + |
| $K_s\pi$ | -0.019 | 0.201 | 0.00 | -140 | - |
| $K\pi\pi$ | -0.051 | 0.190 | 31.9 | -252.9 | + |
| $K\pi\pi$ | -0.004 | 0.221 | 0.00 | -115.2 | + |
| $K_s\pi\pi^o$ | 0.032 | 0.164 | -0.32 | -130.6 | - |
| $K_s\pi\pi\pi$ | 0.001 | 0.245 | -11.7 | -138.9 | + |
| $K\pi\pi\pi^o$ | 0.002 | 0.204 | -8.6 | -88.6 | - |
| $K_s\pi\pi^o$ | 0.014 | 0.208 | -8.3 | -113.0 | + |

TABLE III: Muon Candidate Properties.

use this information and Lorentz transform all laboratory quantities to the center-of-mass. Secondly, we require that the reconstructed $D^-$ have exactly the known $D^-$ mass. This changes and improves somewhat our knowledge of the $D^-$ direction.

The $\text{MM}^2$ from Monte Carlo simulation is shown for our different tagging samples in Fig. 5. The signal is fit to a sum of two Gaussians with the wider Gaussian having about 30% of the area independent of tagging mode. The resolution ($\sigma$) is defined as

$$\sigma = f_1\sigma_1 + (1 - f_1)\sigma_2, \tag{4}$$

where $\sigma_1$ and $\sigma_2$ are the individual widths of the two Gaussians and $f_1$ is the fractional area of the first Gaussian. The resolution is approximately 0.025 $\text{GeV}^2$ consistent among all the tagging decay modes.

We check our simulations using the $D^- \to K_s\pi^-$ decay. Here we choose events with the same requirements as used to search for $\mu^+\nu$ but require one additional found $K_s$. The $\text{MM}^2$ distribution for this final state is shown in Fig. 6. The resolution is measured to be 0.024±0.002 $\text{GeV}^2$ from a single Gaussian fit, consistent with but slightly larger than the Monte Carlo estimate of 0.021±0.001 $\text{GeV}^2$. To account for the difference in resolution between data and simulations we scale the resolution by 14 % to 0.028 $\text{GeV}^2$ when looking for the $D^+ \to \mu^+\nu_\mu$ signal.

The $\text{MM}^2$ distributions for our tagged events requiring no extra charged tracks besides the muon candidate and showers above 250 MeV as described above is shown in Fig. 7. We see a small signal near zero containing 8 events within an interval that is twice as wide as our resolution, -0.056 $\text{GeV}^2$ to +0.056 $\text{GeV}^2$. This signal is most likely due to the $D^+ \to \mu^+\nu_\mu$ mode we are seeking. The large peak centered near 0.25 $\text{GeV}^2$ is from the decay $D^+ \to K^o\pi^+$ that is far from our signal region.

A typical event is shown in Fig. 8.

## VI. BACKGROUND EVALUATION

### A. Introduction

There are several background sources we need to evaluate. These include background from other $D^+$ modes, background from misidentified $D^o\overline{D}^o$ events and continuum background.

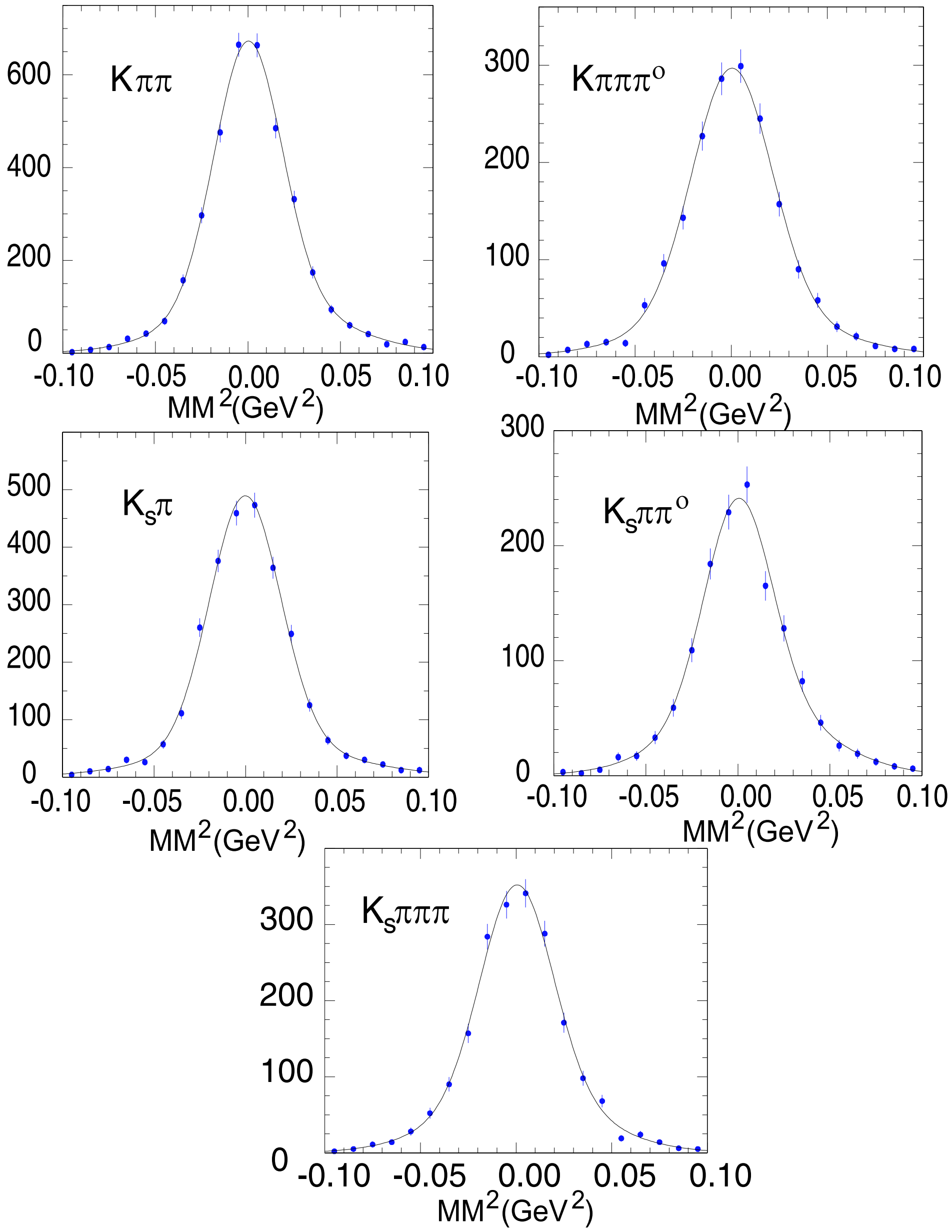


FIG. 5: Monte Carlo simulation of $D^+ \to \mu^+\nu_\mu$ events for different tags. The plots have been fitted to two Gaussians centered at zero where the second Gaussian constitutes around 30% of area.

The requirement of the muon depositing <300 MeV in the calorimeter, while about 99% efficient on muons, rejects only about 40% of pions as determined from the $D^o\overline{D}^o$ event sample where the pion from the $K^{\pm}\pi^{\mp}$ mode was examined. In Fig. 9 we show the deposited energy in the calorimeter for both kaons and pions obtained from the $K\pi$ tag sample.

### B. $D^+$ Backgrounds

There are a few $D^+$ decay modes that could simulate the signal. These are listed in Table IV along with the background estimate we obtained by Monte Carlo generation and

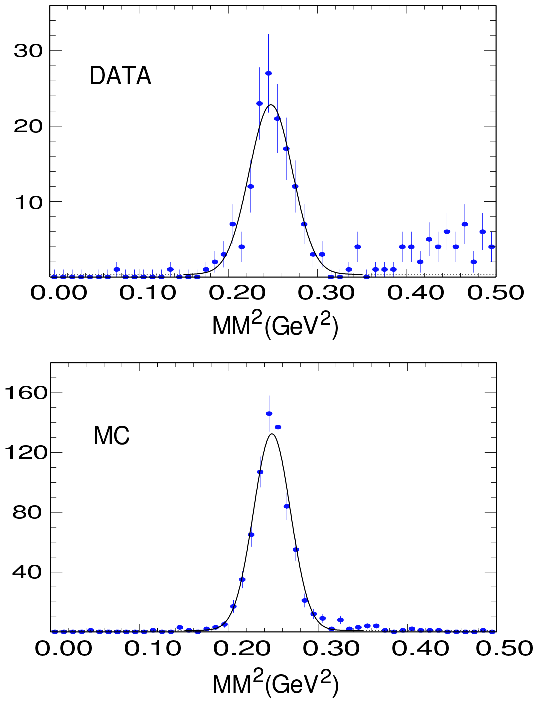


FIG. 6: MM$^2$ distribution for the decay $D^- \to K_s\pi^-$ from data and MC

reconstruction of each specific mode. The branching ratios are from the Particle Data Group except for the $\pi^+\pi^o$ mode where a separate CLEO analysis gives a somewhat lower value [12]. This mode is the most difficult to reject because the MM$^2$ peaks very close to zero, at 0.018 GeV$^2$, well within our resolution of 0.028 GeV$^2$. While we have insisted that the muon candidate be well within our acceptance, it is possible for the photons from the $\pi^o$ decay to inadvertently be matched to the tracks from the tagging $D^-$ or be missed. The maximum photon energy of the $\pi^o$ at the generator level is shown in Fig. 10. We note that at least one photon from the $\pi^+\pi^o$ mode exceeds our 250 MeV calorimeter energy requirement and should in most cases cause such a decay to be vetoed.

Even though the $K^0\pi^+$ mode gives a large peak in the MM$^2$spectrum near 0.025 GeV$^2$, our simulation shows that only a very small amount can enter our signal region, only 0.06 events. We have simulated backgrounds from $D^+ \to \tau^+\nu$. Out of 10,000 simulated events with $D^-$ tags, we found background only when $\tau^+ \to \pi^+\nu$. Because of the small $D^+$-$\tau^+$ mass difference, the $\tau^+$ is almost at rest in the laboratory frame and thus the $\pi^+$ has relatively large momentum causing the MM$^2$ distribution to populate only the low MM$^2$ region, even in this case with two missing neutrinos. The MM$^2$ distribution is shown in Fig. 11.

The semileptonic mode $\pi^o\mu^+\nu_\mu$ is similar to $\pi^+\pi^o$ except that the $\pi^o$ often carries off enough momentum to result in large MM$^2$. We found no candidate background events in a Monte Carlo sample consisting of 50,000 tags plus a $D^+ \to \pi^o\mu^+\nu$ decay.

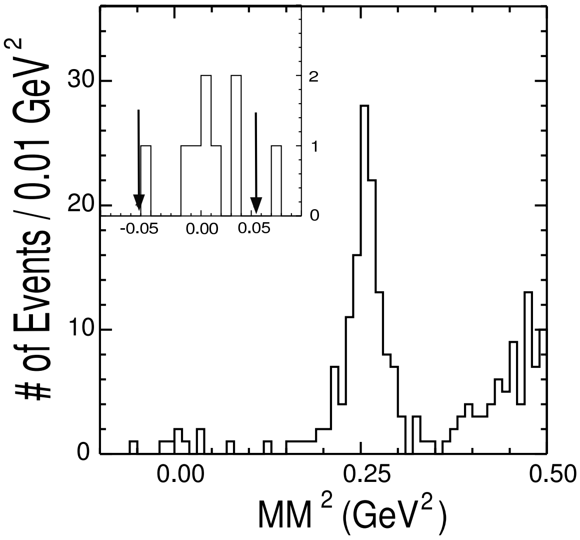


FIG. 7: MM$^2$ using $D^-$ tags and one additional opposite sign charged track and no extra energetic showers (see text). The insert shows the signal region for $D^+ \to \mu^+\nu$ enlarged, $\pm 2\sigma$ range is shown between the two arrows.(preliminary)

| Mode | $\mathcal{B}$ (%) | # of events |
|---|---|---|
| $\pi^+\pi^o$ | 0.13±0.02 | 0.31±0.04 |
| $K^o\pi^+$ | 2.77±0.18 | 0.06±0.05 |
| $\tau^+\nu$ | 3.2× $\mu^+\nu$ | 0.36±0.08 |
| $\pi^o\mu^+\nu$ | 0.31 ± 0.15 | negligible |

TABLE IV: Backgrounds from specific $D^+$ decay modes

### C. $D^o\overline{D}^o$ and Continuum Backgrounds

These backgrounds are evaluated by analyzing Monte Carlo samples corresponding to 15 times the total amount of data in our possession. To normalize our Monte Carlo events to our data sample we used $\sigma_{D^o\overline{D}^o} = 2.9$ nb and $\sigma_{continuum} = 6.4$ nb. In each sample we found one background event within two standard deviations of zero. These correspond to 0.16±0.16 $D^o\overline{D}^o$ events and 0.17±0.17 continuum events forming background.

### D. Background Summary

Our total background is 1.07±0.25 events. Because of the uncertainties in the Monte Carlo simulation we assign a 100% error to our background estimate: 1.07±1.07 events.

## VII. BRANCHING RATIO AND DECAY CONSTANT

Subtracting the 1.07 event background from our 8 events in the signal region, we determine a branching fraction using a detection efficiency for the single muon of 69.9%. This

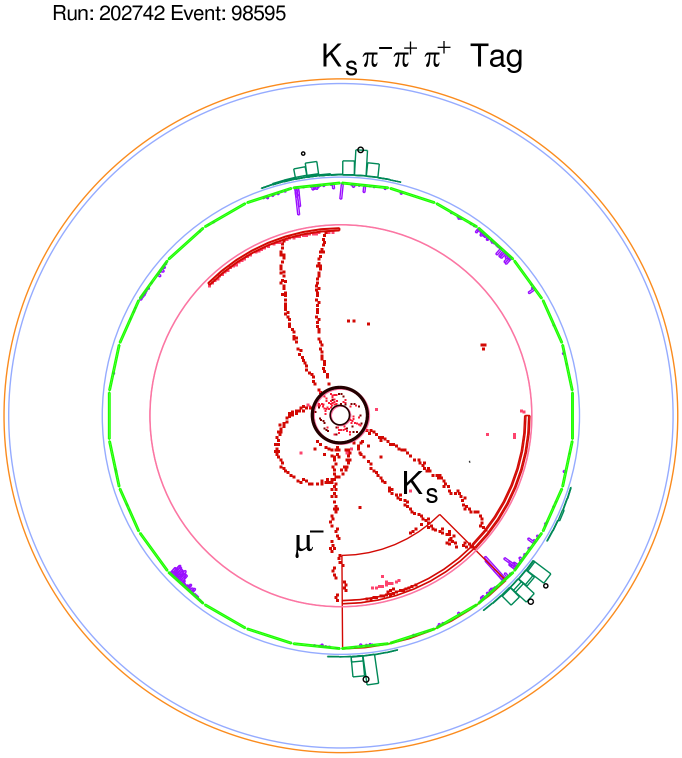


FIG. 8: Typical $D^- \to \mu^- \overline{\nu}_\mu$ event. The muon is shown as well as the two charged pions forming the $K_s$. We notice the presence of a curler track (a pion) with momentum around 50 MeV.

efficiency includes the tracking, the particle identification, the probability of the crystal energy being less than 300 MeV and the probability of not having another unmatched shower in the event with energy greater than 250 MeV. We assign a relative 5.3% error on this efficiency, the components of which are shown in Table V. We use a 3% systematic error on track finding found using the double tagged events and we estimated the error on the particle identification cut to be 1% from studies of $D^{*+}$ decays in higher beam energy data. The error on the minimum ionization cut is evaluated from the efficiency of the cut by generating signal Monte Carlo. To evaluate the error on the extra shower cut we evaluated the efficiency of that cut in the $D^o\overline{D}^o$ sample discussed above. The total systematic error is obtained by summing all entries in quadrature.

To compute the branching ratio we use 6.93 signal events divided by 69.9% and the 28575±286 $D^\mp$ tags. No other efficiencies enter. We find

$$\mathcal{B}(D^+ \to \mu^+\nu_\mu) = (3.5 \pm 1.4 \pm 0.6) \times 10^{-4} \ , \tag{5}$$

The error on the background contributes 15.4% to the systematic error on the branching ratio.

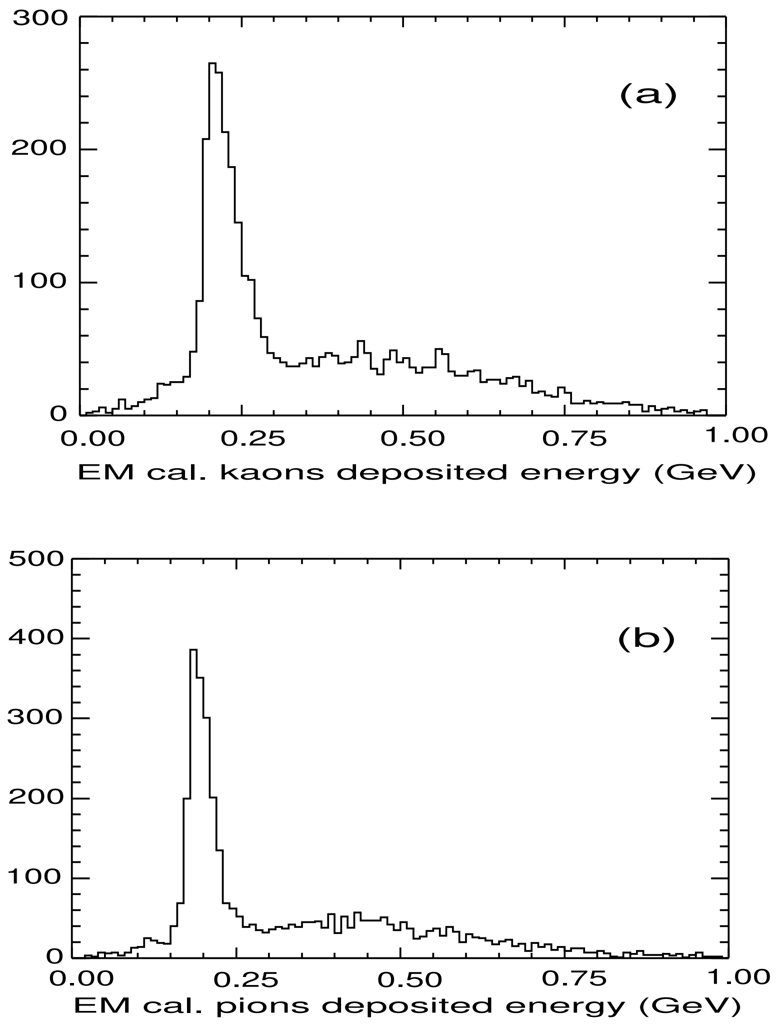


FIG. 9: Deposited energy in EM calorimeter for (a) Kaons, (b) Pions from $D^0 \to K^- \pi^+$.

| | Systematic error % |
|---|---|
| MC statistics | 0.8 |
| Track finding | 3 |
| PID cut | 1 |
| Minimum ionization cut | 1 |
| Extra showers cut | 4 |
| Number of tags | 1 |

TABLE V: Systematic errors on $D^+ \to \mu^+ \nu_\mu$ efficiency.

The decay constant $f_{D^+}$ is then obtained from Equation 1 as

$$f_{D^+} = (201 \pm 41 \pm 17)\ \mathrm{MeV}\ . \tag{6}$$

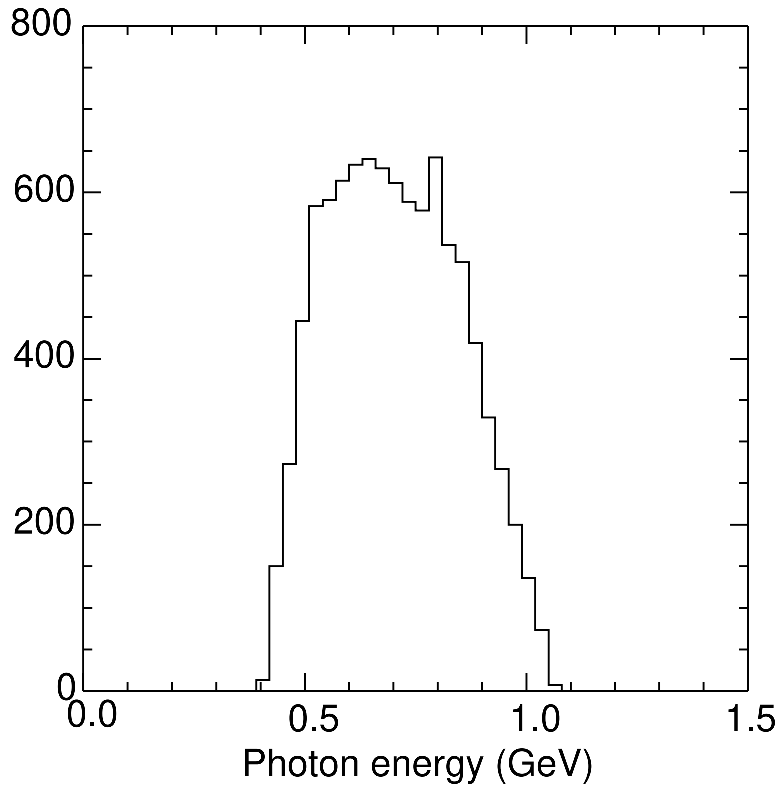


FIG. 10: Maximum photon energy of the $\pi^o$ in the $D^- \to \pi^- \pi^o$ decay.

## VIII. CONCLUSIONS

There have been several experimental studies of $D$ meson decay constants. The Mark III group published an upper limit of $\mathcal{B}(D^+ \to \mu^+ \nu_\mu) < 7.2 \times 10^{-4}$, which leads to an upper limit on the decay constant $f_{D^+} < 290$ MeV at 90% confidence level based on 9.3 pb$^{-1}$ of data taken on the $\psi''$ [13]. BES claimed the observation of one event at a center-of-mass energy of 4.03 GeV with a branching ratio of $(0.08^{+0.17}_{-0.05})\%$ [15]. Recently, using 17.7 pb$^{-1}$ of $\psi''$ data they presented a 3 event signal and claimed a background of 0.25 events where neither $\pi^+\pi^o$, or $\tau^+\nu$ were mentioned as a possible background mode, nor was continuum background considered [16]. Here they find a branching ratio of $(0.12^{+0.092+0.010}_{-0.063-0.009})\%$, and a corresponding value of $f_{D^+} = (365^{+121+32}_{-113-28})$ MeV. Our value is considerably smaller, though compatible with their large error.

Our analysis shows the first statistically compelling signal for $D^+ \to \mu^+\nu$. The preliminary branching fraction is

$$\mathcal{B}(D^+ \to \mu^+\nu) = (3.5 \pm 1.4 \pm 0.6) \times 10^{-4} , \tag{7}$$

and the preliminary decay constant is

$$f_{D^+} = (201 \pm 41 \pm 17) \text{ MeV} . \tag{8}$$

Our result for $f_{D^+}$, at the current level of precision, is consistent with predictions of all of the models listed in Table VI.

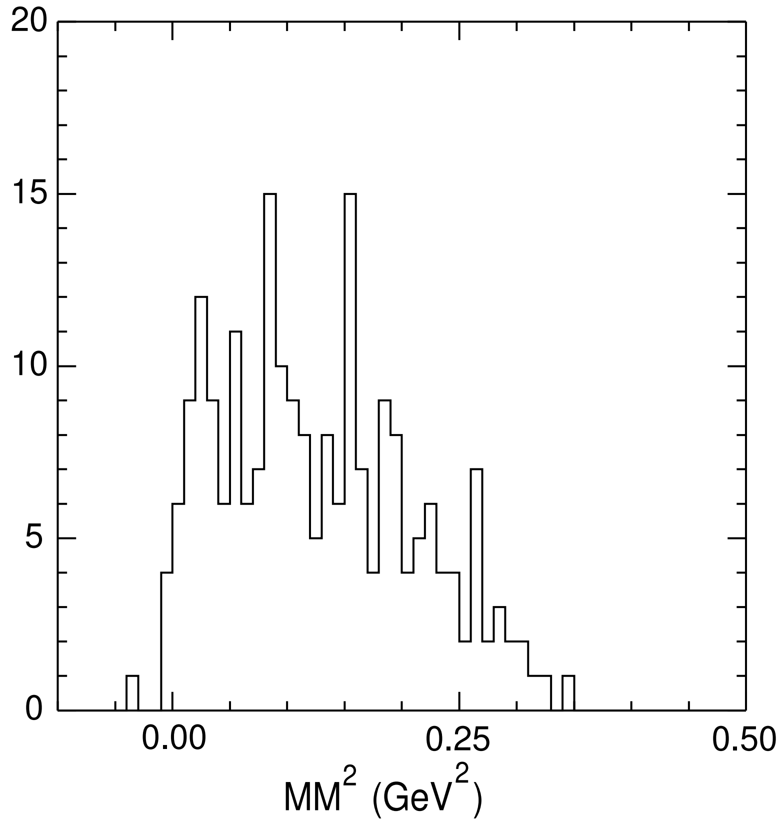


FIG. 11: Missing Mass squared distribution for $D^+ \to \tau^+\nu$ and $\tau^+ \to \pi^+\nu$.

| Model | $f_{D^+}$ (MeV) | $f_{D_s^+}/f_{D^+}$ |
|---|---|---|
| Lattice (unquenched) (UKQCD) [3] | $210 \pm 10^{+17}_{-16}$ | $1.13 \pm 0.02^{+0.04}_{-0.02}$ |
| Lattice (partially quenched) (MILC) [2] | $215 \pm 6^{+16+8+4}_{-15-3-0}$ | $1.14 \pm 0.01^{+0.02}_{-0.03} \pm 0.03 \pm 0.01$ |
| QCD Spectral Sum Rules [5] | $203 \pm 20$ | $1.15 \pm 0.04$ |
| QCD Sum Rules [6] | $195 \pm 20$ | |
| Relativistic Quark Model [7] | $243 \pm 25$ | 1.10 |
| Potential Model [4] | 238 | 1.01 |
| Isospin Mass Splittings [8] | $262 \pm 29$ | |

TABLE VI: Theoretical predictions of $f_{D^+}$ and $f_{D_s^+}/f_{D^+}$

The models generally predict $f_{D_s^+}$ to be 10-15% larger than $f_{D^+}$. CLEO previously measured $f_{D_s^+}$ as $(280 \pm 19 \pm 28 \pm 34)$ MeV [17], and we are consistent with these predictions as well. We look forward to more data to improve the precision.


[1] C. Davies *et al.*, Phys. Rev. Lett. **92**, 022001 (2004) [hep-lat/0304004]; C. Davies, "Lattice QCD," in Heavy Flavour Physics, Scottish Graduate Textbook Series, Institute of Physics 2002, eds C. T. H. Davies and S. M. Playfer [hep-ph/025181]; A. Kron feld, "Heavy Quarks

and Lattice QCD," [hep-lat/0310063].

[2] C. Bernard *et al.* (MILC), Phys. Rev. **D66**, 094501 (2002) [hep-lat/0206016].

[3] L. Lellouch and C.-J. Lin (UKQCD), Phys. Rev. **D64**, 094501 (2001).

[4] Z. G. Wang *et al.*, "Decay Constants of the Pseudoscalar Mesons in the framework of the Coupled Schwinger-Dyson Equation and Bethe-Salpeter Equation," [hep-ph/0403259] (2004); L. Salcedo *et al.*, Braz. J .Phys. **34**, 297 (2004) [hep-ph/0311008].

[5] S. Narison, "Light and Heavy Quark Masses, Flavour Breaking of Chiral Condensates, Meson Weak Leptonic Decay Constants in QCD," [hep-ph/0202200] (2002).

[6] A. Penin and M. Steinhauser, Phys. Rev. **D65**, 054006 (2002).

[7] D. Ebert *et al.*, Mod. Phys .Lett. **A17**, 803 (2002).

[8] J. Amundson *et al.*, Phys. Rev. **D47** 3059 (1993) [hep-ph/9207235].

[9] J. L. Rosner, in **Particles and Fields 3**, Proceed. of the 1988 Banff Summer Inst., Banff, Alberta, Canada, ed. by A. N. Kamal and F. C. Khanna, World Scientific, Singapore, 1989, 395.

[10] K. Hagiwara *et al.* PDG), Phys. Rev. **D66**, 010001 (2002).

[11] M. Artuso *et al.*, Nucl. Instrum. and Meth. **A502**, 91 (2003).

[12] K. Arms *et al.* (CLEO), Phys. Rev. **D69**, 071102 (2004) [hep-ex/0309065].

[13] J. Becker *et al.* (Mark III), SLAC-PUB-4244 (1987).

[14] J. Adler *et al.* (Mark III), Phys. Rev. Lett.60 **1375** (1988).

[15] J. Z. Bai *et al.* (BES), Phys. Lett. B **429**, 188 (1998).

[16] G. Rong, "Recent BES Results on $\psi(3770)$ and D Meson Productions and Decays," presented at XXXIXth Rencontres de Moriond, Electroweak Interactions and Unified Theories, March 2004, [hep-ex/0406027]. It appears that they only consider background modes with muons as they have a muon detector. However, modes with pions could also contribute due to fakes, as the rate for hadrons around 900 MeV faking muons can be quite sizable.

[17] M. Chadha *et al.* (CLEO), Phys. Rev. **D58**, 032002 (1998) [hep-ex/9712014].